



A triangular thick plate finite element with an exact thin limit

F. Auricchio*, R.L. Taylor

Department of Civil Engineering, University of California at Berkeley, Berkeley, CA 94720, USA

Abstract

We present a new formulation for a triangular finite element developed within the framework of a shear deformable plate theory. The element takes advantage of internal rotational degrees of freedom and a *linked* interpolation between the transverse displacement and the rotations. The element has excellent interpolating capacity and presents no locking effects; in fact, the shear energy may be set identically equal to zero without introducing any ill-conditioning, thus recovering a proper thin plate limit.

1. Introduction

In the development of a thick beam finite element the transverse displacement and the rotations are independent kinematic fields; accordingly, independent interpolations are usually assumed. However, if the transverse displacement field is properly *linked* to the nodal rotational degrees of freedom, a constant shear strain within the beam may be represented, hence avoiding locking effects in the limit thin case [1–3]. This approach is however not sufficient in the case of a two dimensional thick plate: in order to avoid locking, or equivalently to satisfy the mixed patch test, we also need to enrich the rotational field with extra modes.

In the present work we consider the interpolations for a triangular element, developed within a shear deformable plate theory. The element has three nodes, uses internal modes for the rotations and linked interpolations for the transverse displacement. Moreover, the element

- has a minimum number of internal degrees of freedom and thus is computationally efficient,
- passes *all* the patch tests,
- shows excellent interpolating capacity,
- is able to exactly solve the thin plate limit case; that is, the matrix from the shear energy may be set identically equal to zero without introducing any ill-conditioning.

* Corresponding author.

The paper is organized as follows. We start with a brief overview of the linear elastic shear deformable plate theory adopted. After that, we introduce a mixed finite element approximation discussing the interpolation requirements. We then describe the finite element and present results from numerical tests.

2. A linear thick plate theory

The thick plate theory presented here is a simplification of the work by Mindlin [4] and Reissner [5]. With the term *plate* we refer to a flat thin body, occupying the domain

$$\Omega = \left\{ (x, y, z) \in \mathcal{R}^3 \mid z \in \left[-\frac{h}{2}, +\frac{h}{2} \right], (x, y) \in \mathcal{A} \subset \mathcal{R}^2 \right\}, \quad (1)$$

where the plane $z = 0$ coincides with the middle surface of the undeformed plate and the transverse dimension, or *thickness* h , is small compared to the other two dimensions. Furthermore, the loading $q(x, y)$ is restricted to the direction normal to the middle surface.

We indicate with w the displacement along the z axis and with $\boldsymbol{\theta} = [\theta_x, \theta_y]^T$ and the rotation of the transverse line element about the x and y axes (refer to [6, Figs. 1.1 and 1.7 of Vol. II]). The curvature, \mathbf{K} , and the shear strain, $\boldsymbol{\Gamma}$, are defined as

$$\mathbf{K} = \begin{Bmatrix} \kappa_{xx} \\ \kappa_{yy} \\ \kappa_{xy} \end{Bmatrix} = \begin{Bmatrix} \theta_{y,x} \\ -\theta_{x,y} \\ \theta_{y,y} - \theta_{x,x} \end{Bmatrix}, \quad (2)$$

$$\boldsymbol{\Gamma} = \begin{Bmatrix} \gamma_{xz} \\ \gamma_{yz} \end{Bmatrix} = \begin{Bmatrix} \theta_y + w_{,x} \\ -\theta_x + w_{,y} \end{Bmatrix}. \quad (3)$$

Assuming $\sigma_z = 0$, integration of the non-zero stresses through the thickness defines the plate stress resultants per unit length:

$$\mathbf{M} = [M_x, M_y, M_{xy}]^T = \left[\int_{-h/2}^{h/2} \sigma_x z \, dz, \int_{-h/2}^{h/2} \sigma_y z \, dz, \int_{-h/2}^{h/2} \tau_{xy} z \, dz \right]^T, \quad (4)$$

$$\mathbf{S} = [S_x, S_y]^T = \left[\int_{-h/2}^{h/2} \tau_{xz} \, dz, \int_{-h/2}^{h/2} \tau_{yz} \, dz \right]^T. \quad (5)$$

Limiting the description to a homogeneous, linearly elastic material, the plate constitutive relation may be written as

$$\begin{Bmatrix} \mathbf{M} \\ \mathbf{S} \end{Bmatrix} = \begin{bmatrix} \mathbf{D}_B & \mathbf{0} \\ \mathbf{0} & \mathbf{D}_S \end{bmatrix} \begin{Bmatrix} \mathbf{K} \\ \boldsymbol{\Gamma} \end{Bmatrix}, \quad (6)$$

where, for isotropy

$$\mathbf{D}_B = D \begin{bmatrix} 1 & \nu & 0 \\ \nu & 1 & 0 \\ 0 & 0 & \frac{1}{2}(1 - \nu) \end{bmatrix}, \quad \mathbf{D}_S = kGh \begin{bmatrix} 1 & 0 \\ 0 & 1 \end{bmatrix}, \quad (7)$$

$$D = \frac{Eh^3}{12(1 - \nu^2)}, \quad G = \frac{E}{2(1 + \nu)}, \quad (8)$$

with E the Young's modulus and ν the Poisson's ratio. Finally, k is a factor, introduced to correct the inconsistency through the thickness between the constant transverse shear strain, and the non-constant shear stress; k depends on the plate properties and is often set equal to $\frac{5}{6}$ for homogeneous plates.

3. Mixed finite element solution

As a starting point, for the development of a mixed finite element scheme, we consider the following functional, described in Refs. [7–9]:

$$\begin{aligned} \Pi(w, \boldsymbol{\theta}, \mathbf{S}) = & \frac{1}{2} \int_A [\mathbf{K}^T(\boldsymbol{\theta}) \mathbf{D}_B \mathbf{K}(\boldsymbol{\theta})] dA \\ & - \frac{1}{2} \int_A [\mathbf{S}^T \mathbf{D}_S^{-1} \mathbf{S}] dA + \int_A [\mathbf{S}^T (\nabla w + \mathbf{e} \boldsymbol{\theta})] dA + \Pi_{\text{ext}}, \end{aligned} \quad (9)$$

where Π_{ext} describes loading and boundary effects. Following a *mixed* approach, we approximate the fields w , $\boldsymbol{\theta}$ and \mathbf{S} with independent interpolation schemes; in particular, we link the transverse displacement field to the discrete rotational parameters and enrich the rotational field with internal degrees of freedom (d.o.f). Accordingly, we have

$$w = N_w \hat{w} + N_{w\theta} \hat{\boldsymbol{\theta}}, \quad \boldsymbol{\theta} = N_\theta \hat{\boldsymbol{\theta}} + N_b \hat{\boldsymbol{\theta}}_b, \quad \mathbf{S} = N_S \hat{\mathbf{S}}, \quad (10)$$

where: \hat{w} , $\hat{\boldsymbol{\theta}}$ are the d.o.f of the discretized system associated with the boundary vertex nodes; $\hat{\boldsymbol{\theta}}_b$, $\hat{\mathbf{S}}$ are, respectively, the internal rotational d.o.f and the shear stress d.o.f;

$$N_w, N_{w\theta}, N_\theta, N_b, N_S$$

are sets of shape functions, where N_b are bubble modes and $N_{w\theta}$ are *linked* interpolations chosen such to make the transverse shear strain constant along each side of the finite element [1, 2]. Using the interpolation scheme described in Eq. (10), we guarantee the following:

- a higher order complete polynomial in the transverse displacement interpolation than in the rotational field interpolation, as is required for the thin plate situation when the rotations are simply the derivative of the displacements;
- a transverse displacement interpolation with as few nodal parameters as possible and a larger number of rotational parameters, as required for the satisfaction of the mixed patch test [6].

The stationary condition for the functional leads to the following algebraic system:

$$\begin{bmatrix} \mathbf{K}_{UU} & \mathbf{K}_{US} & \mathbf{K}_{Ub} \\ \mathbf{K}_{US}^T & \mathbf{K}_{SS} & \mathbf{K}_{Sb} \\ \mathbf{K}_{Ub}^T & \mathbf{K}_{Sb}^T & \mathbf{K}_{bb} \end{bmatrix} \begin{Bmatrix} \hat{\mathbf{U}} \\ \hat{\mathbf{S}} \\ \hat{\boldsymbol{\theta}}_b \end{Bmatrix} = \begin{Bmatrix} \mathbf{f}_U \\ \mathbf{0} \\ \mathbf{0} \end{Bmatrix}, \quad (11)$$

where $\hat{\mathbf{U}} = [\hat{\boldsymbol{\psi}}, \hat{\boldsymbol{\theta}}]$ are the vertex d.o.f. A detailed description of system (11) can be found in Ref. [8]. If we first eliminate the internal rotational d.o.f and then the shear parameters, we get the following stiffness matrix:

$$[\mathbf{A}_{UU} - \mathbf{A}_{US} \mathbf{A}_{SS}^{-1} \mathbf{A}_{US}^T] \hat{\mathbf{U}} = \mathbf{f}_U, \quad (12)$$

where

$$\begin{aligned} \mathbf{A}_{UU} &= [\mathbf{K}_{UU} - \mathbf{K}_{Ub} (\mathbf{K}_{bb})^{-1} \mathbf{K}_{Sb}^T], \\ \mathbf{A}_{SS} &= [\mathbf{K}_{SS} - \mathbf{K}_{Sb} (\mathbf{K}_{bb})^{-1} \mathbf{K}_{Sb}^T], \\ \mathbf{A}_{US} &= [\mathbf{K}_{US} - \mathbf{K}_{Ub} (\mathbf{K}_{bb})^{-1} \mathbf{K}_{Sb}^T]. \end{aligned} \quad (13)$$

Note that we are never required to invert \mathbf{K}_{SS} . On the other hand, we are required to invert \mathbf{A}_{SS} and we may guarantee its invertibility by an appropriate choice of the N_b interpolating functions. In particular, we desire \mathbf{A}_{SS} to be invertible also for the case of \mathbf{K}_{SS} identically equal to zero, which is the thin plate limit. Accordingly, if such judicious choice of the N_b function is performed, then

- we may always solve a sequence of problems converging to the thin plate case,
- depending on the purposes of the analysis, the shear energy may be arbitrarily included or excluded (setting $\mathbf{K}_{SS} = \mathbf{0}$), without the problem becoming ill-conditioned,
- we may always recover the shear parameters $\hat{\mathbf{S}}$, even for the case in which the shear energy is excluded.

Elements which satisfy the above conditions require no ad hoc assumptions (e.g., energy balancing) to solve thin plate problems. Finally, note that some of the elements presented in the literature may be reinvestigated, taking into consideration the discussion in this section.

4. A thick plate finite element

Due to the element geometry, the shape functions are expressed in terms of the area coordinates L^i ($i = 1, 2, 3$) [6, 10]. Accordingly, the region occupied by each element may be expressed as

$$\mathbf{x} = \sum_{i=1}^3 L^i \mathbf{x}^i,$$

where $\mathbf{x} = \{x, y\}^T$ is any point in the element and $\mathbf{x}^i = \{x^i, y^i\}^T$ are the nodal coordinates.

The transverse displacement interpolation is linear in the nodal parameters \hat{w}^i , enriched with linked quadratic functions expressed in terms of the nodal rotations $\hat{\theta}$:

$$w = N_w \hat{w} + N_{w\theta} \hat{\theta} = \sum_{i=1}^3 L^i \hat{w}^i - \frac{1}{2} \sum_{i=1}^3 L^i L^j (\hat{\theta}_n^i - \hat{\theta}_n^j) l^k, \quad (14)$$

where l^k is the i - j side length, $\hat{\theta}_n^i$ and $\hat{\theta}_n^j$ are the components of the rotations of i and j nodes in the direction normal to the i - j side.

The rotational field interpolation is linear in the nodal parameters $\hat{\theta}^i$, enriched with two internal d.o.f $\hat{\theta}_b$ associated with a bubble functions:

$$\theta = N_\theta \hat{\theta} + N_b \hat{\theta}_b = \sum_{i=1}^3 L^i \hat{\theta}^i + 27 L^1 L^2 L^3 [\hat{\theta}_b^1, \hat{\theta}_b^2]^T. \quad (15)$$

The shear is assumed constant within the element:

$$\mathbf{S} = \hat{\mathbf{S}} = [\hat{S}^1, \hat{S}^2]^T. \quad (16)$$

Due to the fact that $\hat{\theta}_b$ and $\hat{\mathbf{S}}$ are quantities local to each element, the matrix condensation presented in Section 3 may be performed at the element level. In the following we will refer to this element as T3-2LIM (Triangular element with 3 nodes, 2 bubble modes, based on Linked interpolation and a Mixed approach).

5. Numerical examples

The element has been implemented into the Finite Element Analysis Program (FEAP) [6]. Its numerical performance is compared with analytical or series solutions or with other elements available in the literature. As benchmark elements, we choose the quadrilateral Q4-LIM [8] and the quadrilateral T1 [10]; the results reported for these elements are computed using the finest mesh for which results from the T3-2LIM element are presented.

5.1. Patch test

The first part of the mixed patch test [6] is used to determine solvability of the algebraic system presented in Eq. (11), when $\mathbf{K}_{SS} = \mathbf{0}$. For the present formulations this test is expressed as

$$n_\theta + n_b + n_w \geq n_s, \quad n_s \geq n_w, \quad (17)$$

where n_w , n_θ , n_b and n_s stand for the number of d.o.f for \hat{w} , $\hat{\theta}$, $\hat{\theta}_b$ and $\hat{\mathbf{S}}$, respectively [8]. The T3-2LIM element has two internal rotational d.o.f and two shear parameters, accordingly $n_b = n_s$ and Eq. (17)₁ is satisfied a priori. The second algebraic requirement is checked on different meshes and also is always satisfied. Since this constraint count is just a necessary condition for the stability of the formulation, an eigen-analysis on the stiffness matrix after condensation is performed for patches of one or more elements. We consider a thick ($L/h = 10$) and very thin plate ($L/h = 100\,000$), and the bending stiffness is kept constant while reducing the thickness. In the single element test, there is one extra zero eigenvalues; however, in any multi-element mesh the number of zero eigenvalues

equals the number of rigid body motions, thus, the extra zero energy mode does not communicate between elements. In Table 1 we report the eigenvalues for a single element test, both for the case with shear energy ($\mathbf{K}_{SS} \neq \mathbf{0}$) and for the case without shear energy ($\mathbf{K}_{SS} = \mathbf{0}$). It is interesting to observe that no eigenvalue tends to zero or to infinity in the limit thin case and that for the analysis of thick plates without shear energy we recover exactly the eigenvalues of the thin limit case.

To assess consistency, the ability to exactly reproduce constant bending, twisting, shear strain states is tested for a thick and a thin case ($L/h = 10$ and $L/h = 1000$). To investigate possible pathologies in the limiting thin case, the bending stiffness is kept constant during the curvature test, while the shear stiffness is kept constant during the constant shear strain test. The T3-2LIM element passes all consistency tests.

5.2. Cylindrical bending of simply supported strip

In this example we check the ability of the element to perform analysis including or excluding the shear energy. We consider a simply supported strip with $L/h = 1$; although outside the range of application for the plate theory presented in Section 2, this ratio L/h permits comparison of numerical and exact solution. The material properties are: $E = 1000$, $\nu = 0$. The strip is constrained to produce cylindrical bending and is loaded in the midspan with a concentrated force $F = 400$ per unit length of the cross section. Accordingly, the vertical displacements due to bending and shear are given by:

$$w_b\left(\frac{L}{2}\right) = \frac{FL^3}{48D} = 0.10, \quad w_s\left(\frac{L}{2}\right) = \frac{3FL}{10Gh} = 0.24$$

for a total displacement of $w_{\text{tot}} = w_b + w_s = 0.34$. In Table 2, we report the numerical response of the T3-2LIM element in terms of vertical displacement, moment and shear for the case with and without shear energy. In Fig. 1, we also plot the deformed configuration of the strip for both cases.

Table 1
Single element eigenvalues. A thick ($L/h = 10$) and a thin ($L/h = 100000$) plate are considered, with and without shear energy ($\mathbf{K}_{SS} \neq \mathbf{0}$ and $\mathbf{K}_{SS} = \mathbf{0}$, respectively).

Thick	$\mathbf{K}_{SS} \neq \mathbf{0}$	6.0727E+00	2.7776E+00	1.5629E+00
		5.6662E-01	2.9398E-01	3.1933E-16
		-1.8273E-16	-3.2133E-17	1.5641E-17
	$\mathbf{K}_{SS} = \mathbf{0}$	6.3960E+00	2.8640E+00	1.5638E+00
		5.6766E-01	2.9436E-01	-6.8628E-16
		-3.5539E-16	-1.3075E-17	-8.3921E-18
Thin	$\mathbf{K}_{SS} \neq \mathbf{0}$	6.3960E+00	2.8640E+00	1.5638E+00
		5.6766E-01	2.9436E-01	-3.8124E-16
		2.5050E-16	-1.3791E-17	3.7348E-18
	$\mathbf{K}_{SS} = \mathbf{0}$	6.3960E+00	2.8640E+00	1.5638E+00
		5.6766E-01	2.9436E-01	-6.8628E-16
		-3.5539E-16	-1.3075E-17	-8.3921E-18

Table 2
Simply supported strip

Mesh	T3-2LIM				T1		
	w_b	w_s	w_{tot}	M	S	w_{tot}	M
1×10	1.0000	2.4000	3.4000	957	200	3.3975	950
1×50	1.0000	2.4000	3.4000	991	200	3.3999	990
1×100	1.0000	2.4000	3.4000	996	200	3.4000	995
Ex.sol	1.0000	2.4000	3.4000	995	200	3.4000	995

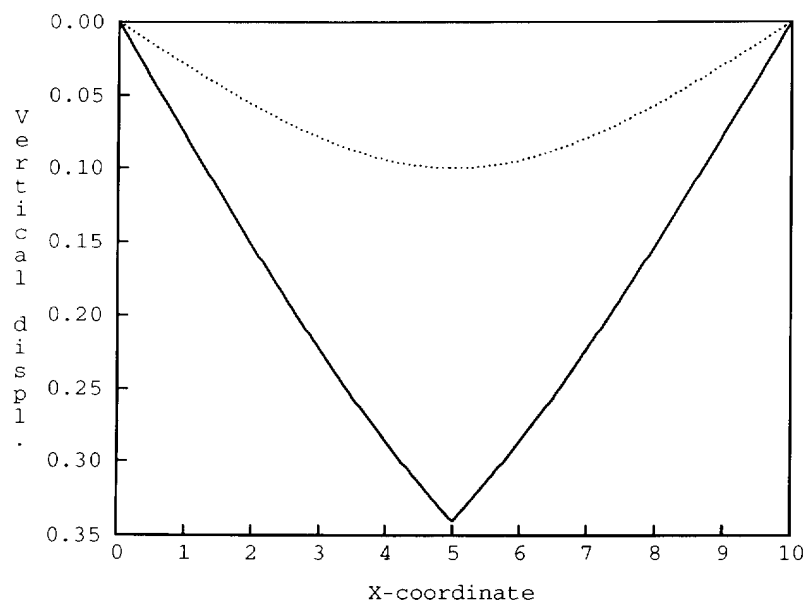


Fig. 1. Simply supported strip. Vertical displacement for the strip with shear energy (continuous line) and without shear energy (dotted line).

5.3. Simply supported square plate

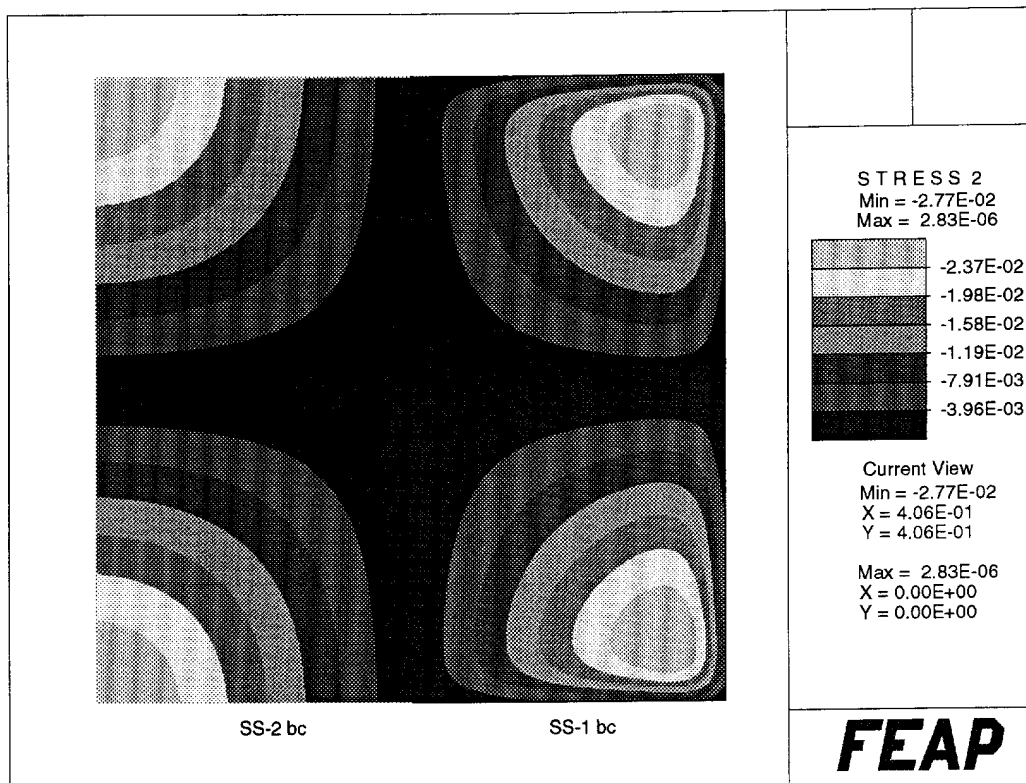
Both a thick ($L/h = 10$) and a thin plate ($L/h = 1000$) are considered, where L is the side length and h the thickness, with load $q = 1$ and material properties $E = 10.92$, $\nu = 0.3$. The numerical results are presented in Table 3, together with the Navier series solution. Both the SS-1 (zero twist moment) and the SS-2 (zero twist rotation) boundary conditions are considered for the thick plate [6, 10]. To highlight the influence of the boundary condition on the plate response, contours for the twist moment M_{xy} are shown in Fig. 2 for the thick plate with SS-1 and SS-2 boundary.

For a plate with no shear energy, we plot in Fig. 3 the contour of the shear S_x obtained from a finite element analysis (left side) and from a series solution (right side). It is evident that for the thin plate case high accuracy for shears can be attained using the T3-2LIM element.

Table 3

Simply supported square plate: displacement and moment at the center (thick plate, $L/h = 10$; thin plate: $L/h = 1000$)

Mesh	Thick (SS-1)		Thick (SS-2)		Thin (SS-2)	
	$w/(qL^4/100D)$	$M/(qL^2/100)$	$w/(qL^4/100D)$	$M/(qL^2/100)$	$w/(qL^4/100D)$	$M/(qL^2/100D)$
2 × 2	0.44212	4.4132	0.40786	4.0918	0.38412	4.0831
4 × 4	0.44693	4.8263	0.42293	4.6063	0.40114	4.6071
8 × 8	0.45440	4.9929	0.42627	4.7398	0.40503	4.7408
16 × 16	0.45923	5.0633	0.42704	4.7755	0.40594	4.7759
32 × 32	0.46101	5.0868	0.42723	4.7852	0.40616	4.7853
Q4 – LIM	0.46144	5.0922	0.42728	4.7874	0.40623	4.7874
T1	0.46127	5.0904	0.42726	4.7868	0.40621	4.7868
Series	—	—	0.42728	4.7886	0.40624	4.7886

Fig. 2. Thick simply supported plate: M_{xy} moment for SS-2 boundary condition (left side) and SS-1 boundary condition (right side).

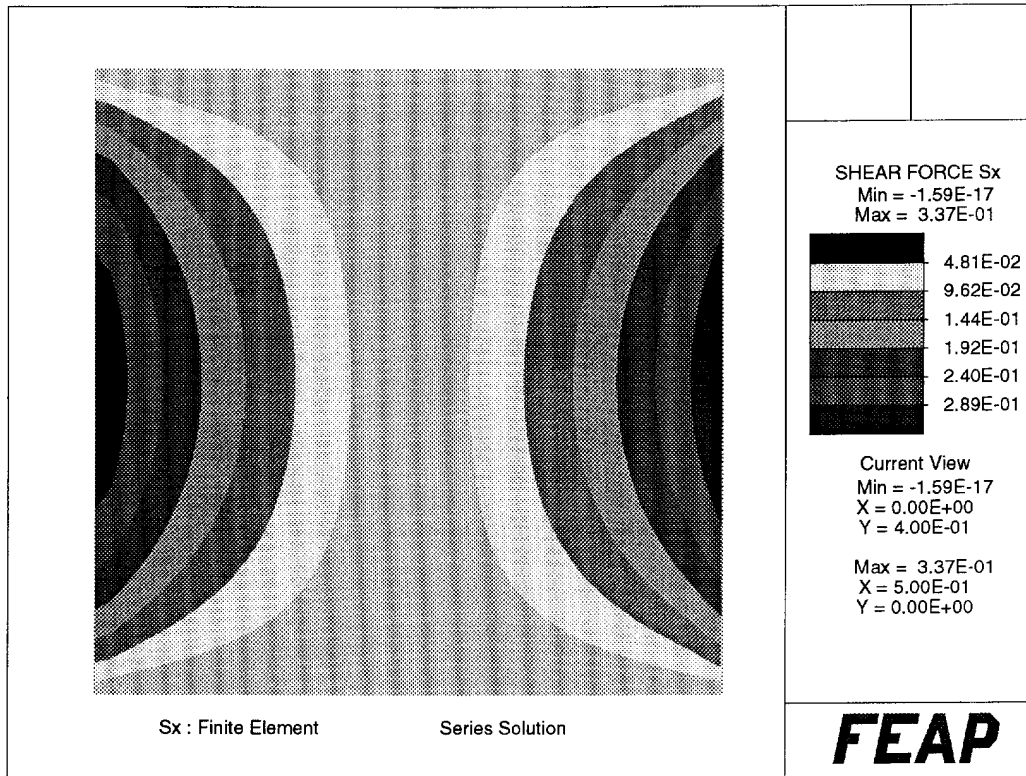


Fig. 3. Thin simply supported (SS-2) plate: S_x shear. Finite element solution (left side) versus series solution (right side).

In Fig. 4 we plot the vertical displacement for the SS-2 boundary condition for a wide range of thickness versus side length values. The results from the T1 element are also reported for comparison. The ability of the new element to analyze very thin plates is clearly evident.

5.4. Simply supported skew plate

We consider a highly skewed plate ($\beta = 60^\circ$), simply supported along all boundaries. The plate has unit load q , side length $L = 100$ and two thicknesses are considered, e.g., $h = 1$ and $h = 0.1$. The material properties are: $E = 10.92$, $\nu = 0.3$. The displacement and the two principal bending moments at the center of the plate are reported in Table 4. In addition, in Fig. 5 we test the element performance in terms of energy, as suggested by Babuska and Scapolla [11]. The properties used are $E = 3.0E7$, $\nu = 0.3$, with $h = 0.01$, $L = 1$ and $q = 1$.

The excellent performance of the element on the skew plate problems is particularly noted.

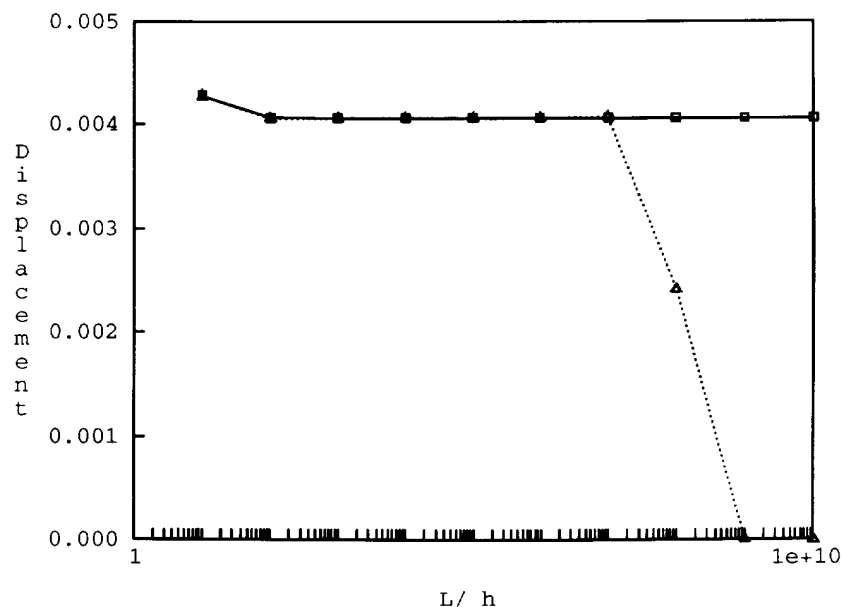


Fig. 4. Simply supported (SS-2) square plate: displacement versus L/h . The results from the T3-2LIM element are represented with a continuous line; the results from the T1 element are represented with a dotted line.

Table 4

Simply supported skew plate (soft boundary): displacement and moments at the center (thick plate, $L/h = 100$; thin plate, $L/h = 1000$)

Mesh	Thick			Thin		
	$w/(qL^4/100D)$	$M_2/(qL^2/100)$	$M_1/(qL^2/100)$	$w/(qL^4/100D)$	$M_2/(qL^2/100)$	$M_1/(qL^2/100)$
2×2	0.63591	0.9207	1.7827	0.63508	0.9204	1.7827
4×4	0.45819	1.0376	1.8543	0.45724	1.0372	1.8532
8×8	0.43037	1.1008	1.9254	0.42922	1.0999	1.9247
16×16	0.42382	1.1233	1.9416	0.42188	1.1200	1.9376
32×32	0.42183	1.1284	1.9439	0.41816	1.1186	1.9344
Q4 – LIM	0.42178	1.1263	1.9440	0.41363	1.1008	1.9209
T1	0.40383	1.0701	1.8897	0.36156	0.9153	1.7689

6. Closure

In the present paper we present a triangular finite element developed within the framework of a shear deformable plate theory. The element takes advantage of internal rotational degrees of freedom and *linked* interpolation between the transverse displacement and the rotational field. The advantages of this approach can be summarized as follows:

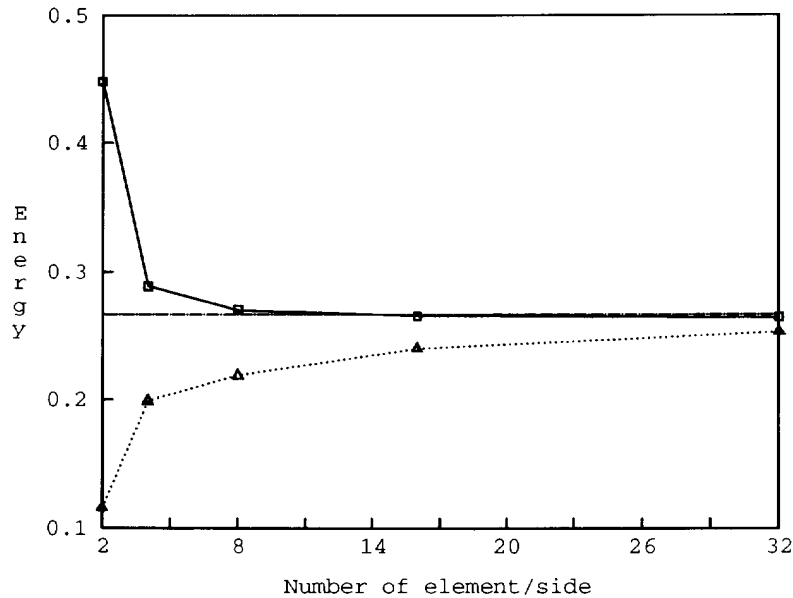


Fig. 5. Simply supported (SS-1) skew plate: energy versus number of element per side. The results from the T3-2LIM element are represented with a continuous line; the results from the T1 element are represented with a dotted line.

- with an appropriate choice of the $N_{w\theta}$ shape functions we are able to obtain a constant shear strain along each side of an element,
- we guarantee a higher order complete interpolation for the transverse displacement than for the rotational field, as is required for the thin plate situation, where the latter are simply the derivative of the former,
- we have a transverse displacement interpolation with as few nodal parameters as possible and we have a larger number of rotational parameters, as required by the mixed patch test.

The element has excellent accuracy and no locking effects in the limiting case of a thin plate; in fact, due to the particular order adopted for the condensation of the internal parameters for each element, we may

- solve a sequence of problems converging to the thin plate case,
- arbitrarily include or exclude the shear energy (setting $\mathbf{K}_{SS} = \mathbf{0}$), without introducing any ill-conditioning,
- always recover the shear parameters $\hat{\mathbf{S}}$, even for the case in which the shear energy is excluded.

References

- [1] M.A. Crisfield, *Finite elements and solution procedures for structural analysis, Vol. I: Linear analysis*, Pineridge Press, Swansea, UK, 1986.
- [2] R.L. Taylor, Finite element analysis of linear shell problems, in: J. Whiteman, (ed.), *MAFELAP 1987: The Mathematics of Finite Elements and Applications VI* Academic Press, New York, 1987.

- [3] A. Tessler and S.B. Dong, On a hierarchy of conforming Timoshenko beam elements, *Comput. Struct.* **14**, pp. 335–344, 1981.
- [4] R.D. Mindlin, Influence of rotatory inertia and shear in flexural motion of isotropic, elastic plates, *J. Appl. Mech.* **18**, pp. 31–38, 1951.
- [5] E. Reissner, The effect of transverse shear deformation on the bending of elastic plates, *J. Appl. Mech.* **12**, pp. 69–76, 1945.
- [6] O.C. Zienkiewicz and R.L. Taylor, *The Finite Element Method*, Vol. I and II, McGraw-Hill, New York, 1991.
- [7] F. Auricchio and R.L. Taylor, 3-node triangular elements based on Reissner–Mindlin plate theory, Report UCB/SEMM-91/04, Department of Civil Engineering, University of California at Berkeley, 1991, Copies available through NISEE. E-mail: nisee@cmsa.berkeley.edu.
- [8] F. Auricchio and R.L. Taylor, A shear deformable plate element with an exact thin limit, *Comput. Methods Appl. Mech. Eng.* **118**, pp. 393–412, 1994.
- [9] O.C. Zienkiewicz, Z. Xu, L.F. Zeng, A Samuelsson and N.E. Wiberg, Linked interpolation for Reissner–Mindlin plate elements: Part I: a simple quadrilateral, *Int. J. Numer. Methods Eng.* **36**, pp. 3043–3056, 1993.
- [10] T.J.R. Hughes, *The Finite Element Method*, Prentice Hall, Englewood Cliffs, NJ, 1987.
- [11] I. Babuska and T. Scapolla, Benchmark computation and performance evaluation for rhombic plate bending problems, *Int. J. Numer. Methods Eng.* **28**, pp. 155–179, 1989.